

Electronic Supplementary Information (ESI):

Synthesis and photocatalytic activity of porous anatase TiO₂ microspheres composed of {010}-faceted nanobelts

Jun Zhao, Xiao-Xin Zou,* Juan Su, Pei-Pei Wang, Li-Jing Zhou, Guo-Dong Li*

State Key Laboratory of Inorganic Synthesis and Preparative Chemistry, Jilin University, Changchun 130012, P.R. China

* E-mail: G. D. Li, lgd@jlu.edu.cn;

X. X. Zou, chem_zouxx@163.com

Experimental Section

Materials: Titanium (IV) isopropoxide (TTIP) was purchased from Shanghai D&R Finechem Co. Ltd. Isopropanol, methanol, ethanol, butanol and hexanol were purchased from Beijing Chemical Works. Glycerol was purchased from Sinopharm Chemical Reagent Co. Ltd. Titania P25 with a BET surface area of about $50 \text{ m}^2 \text{ g}^{-1}$ was purchased from Beijing Entrepreneur Science & Trading Co. Ltd. All the above chemicals were used without further purification and deionized water was used in all experiments.

Preparation of TG-1 and TG-2: For the synthesis of TG-1, TTIP (5.0 mmol) was dispersed in a mixed solution of glycerol (20 mL) and isopropanol (20 mL). The resulting mixture was stirred at room temperature. After stirring for 10 min, the clear solution was transferred into a 60 mL Teflon-Lined autoclave, which was treated at $180 \text{ }^\circ\text{C}$ for 16 h. After cooled to room temperature, the white precipitate was washed several times with deionized water and ethanol, and dried in an oven overnight at $80 \text{ }^\circ\text{C}$ in air. The obtained solid product was labeled as TG-1. For comparison, other supporting solvents, such as ethanol, butanol and hexanol, with the same quantity were used to replace isopropanol (see SEM images in Fig. S7).

For the synthesis of TG-2, TTIP (5.0 mmol) was dispersed in glycerol (40 mL) and stirred at room temperature. After stirring for 10 min, the clear solution was transferred into a 60 mL Teflon-Lined autoclave, which was also treated at $180 \text{ }^\circ\text{C}$ for 16 h. After cooled to room temperature, the white precipitate was washed several times with deionized water and ethanol, and dried in an oven overnight at $80 \text{ }^\circ\text{C}$ in air. The obtained solid product was labeled as TG-2.

Preparation of TiO₂-1 and TiO₂-2: TiO₂-1 and TiO₂-2 were obtained by calcining the TG-1 and TG-2 in a muffle furnace at $450 \text{ }^\circ\text{C}$ for 4 h, respectively.

General Characterization: The powder X-ray diffraction (XRD) patterns were recorded on a Rigaku D/Max 2550 X-ray diffractometer using $\text{Cu}_{\text{K}\alpha}$ radiation ($\lambda = 1.5418 \text{ \AA}$) operated at 200 mA and 50 kV. The scanning electron microscopic (SEM) images were recorded on a JEOL JSM 6700F electron microscope. The transmission electron microscopy (TEM) and high-resolution TEM (HRTEM) images were obtained on a Philips-FEI Tecnai G2S-Twin with a field emission gun operating at 200 kv. The Brunauer-Emmett-Teller surface areas and Nitrogen adsorption-desorption isotherms of the samples were measured by using a Micromeritics ASAP 2020M system. The infrared (IR) spectra were recorded on a Bruker IFS 66V/S FTIR spectrometer using KBr pellets. The thermal gravimetric analysis curve was recorded on a NETZSCH STA 449C TG thermal analyzer from 25 to $800 \text{ }^\circ\text{C}$ at a heating rate of $10 \text{ }^\circ\text{C min}^{-1}$ in air. The UV/Vis diffuse reflectance spectra were recorded on a Perkin-Elmer Lambda 20 UV/Vis spectrometer. Photoluminescence (PL) measurements were carried out at room temperature with a fluorescence spectrometer

(Perkin-Elmer LS55), using a 290 nm excitation wavelength. The X-ray photoelectron spectroscopy (XPS) was performed on an ESCALAB 250 X-ray photoelectron spectrometer with a monochromated X-ray source (Al KR $h\nu = 1486.6$ eV). The energy scale of the spectrometer was calibrated using Au4f_{7/2}, Cu2p_{3/2}, and Ag3d_{5/2} peak positions. The standard deviation for the binding energy (BE) values was 0.1 eV.

Evaluation of photocatalytic activity: The photocatalytic activities of these samples were evaluated by photocatalytic H₂ evolution under UV-light irradiation. The photocatalytic reaction was performed in a quartz cell, which was connected with a closed gas circulation system and irradiated from an external light source. The UV-light source was a 125 W high-pressure Hg lamp. The main emission wavelength is 365 nm and the light intensity is about 20 mW/cm².

A photocatalyst (25 mg) was added into aqueous methanol solution (50 vol %, 50 mL) in the cell and the aqueous system was magnetically stirred during the whole photocatalytic testing. Pt co-catalyst was loaded onto the surface of the photocatalyst by an *in situ* photo-deposition method using an appropriate amount of H₂PtCl₆·6H₂O as precursor. Before light irradiation, the system was evacuated to eliminate air and the temperature of the system during photocatalytic reaction was kept around 23 °C by a continuous flow of water. The evolved gases were detected *in situ* using an online gas chromatograph (Shimadzu, GC-2014C, TCD, Molecular sieve 5 Å, Argon gas), which was connected to the system and was equipped with a thermal conductivity detector.

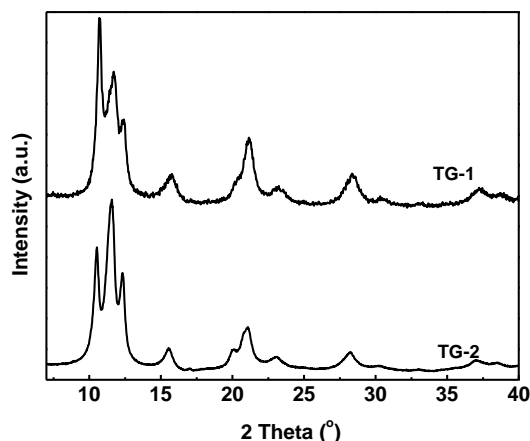


Fig. S1 XRD patterns of TG-1 and TG-2. From Fig. S1, it is seen that the XRD patterns of TG-1 and TG-2, which are similar to that of previously-reported titanium glycerolate. Although isopropanol as supporting solvent was introduced deliberately into the reaction system, crystal structure of titanium glycerolate is not changed by the addition of isopropanol. However, isopropanol may be adsorbed on the crystal surfaces of titanium glycerolate particles, and thus inhibits the growth of some facets of the latter and lead to the great change of XRD peak intensities.

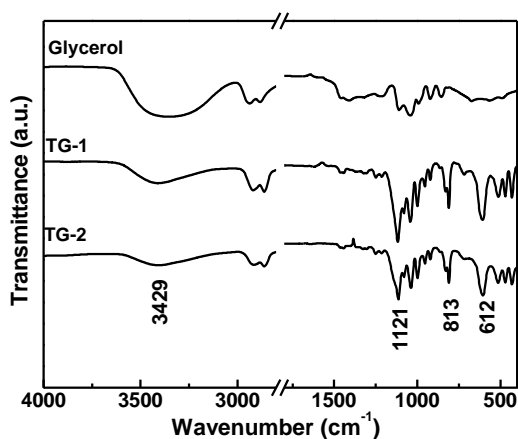


Fig. S2 IR spectra of glycerol, TG-1 and TG-2. The IR spectra of TG-1 and TG-2 are almost same. Compared to that of glycerol, the IR spectrum of TG-1 or TG-2 shows that the IR absorption band of OH groups at 3429 cm^{-1} is weakened, whereas several IR absorption peaks between 1121 and 813 cm^{-1} , which are generally assigned to C-C-O and C-O-Ti groups, are strengthened. More importantly, some new absorption peaks below 612 cm^{-1} , which are not observed in IR spectrum of glycerol, show up in IR spectrum of TG-1 or TG-2, and they are assigned to the stretching and bending vibrations of Ti-O and Ti-O-Ti groups. The above IR features indicates that the glycerolate ligands indeed link to titanium atoms to form TG-1/TG-2 compound.

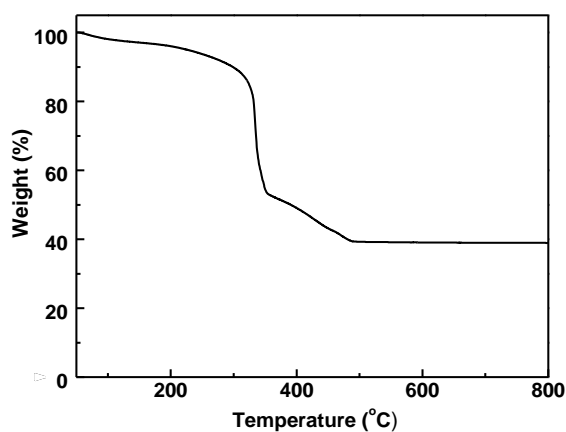


Fig. S3 The TG curve measured in air for TG-1. From the weight loss values it is estimated that the empirical composition of TG-1 is $\text{Ti}_3(\text{C}_3\text{H}_5\text{O}_3)_4$. And C/H/N elemental analysis further confirms the chemical composition of TG-1. 30.4 wt % carbon and 5.0 wt % hydrogen in TG-1 were detected, in agreement with the calculated results (C 29.0 wt %; H 4.0 wt %).

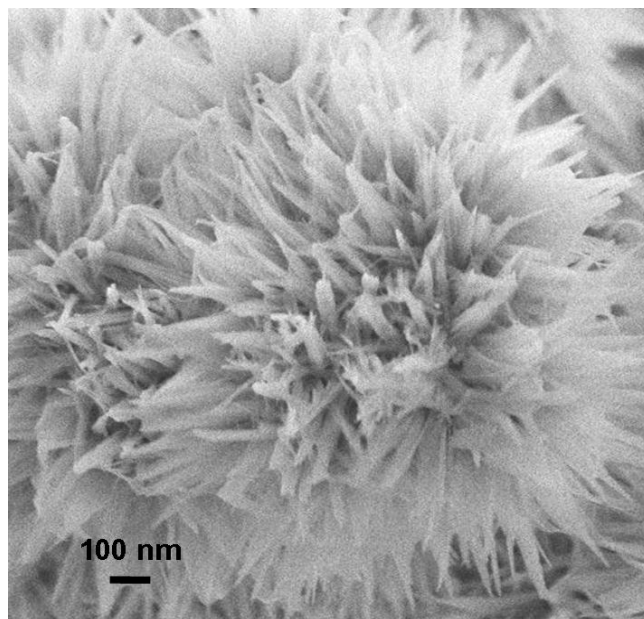


Fig. S4 High-magnification SEM image of TG-1.

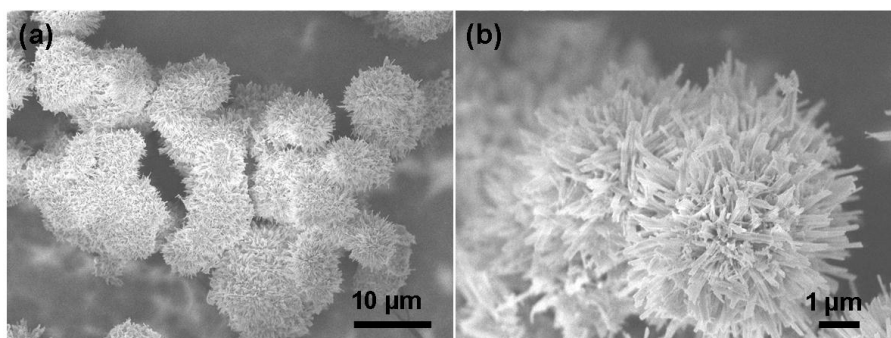


Fig. S5 SEM images of TG-2.

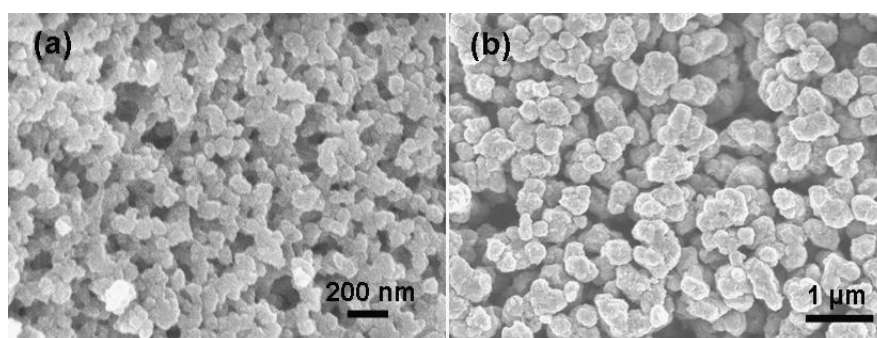


Fig. S6 Comparison of crystal nucleus of TG-1 (a) and TG-2 (b). The SEM images of two typical samples obtained after reaction for 1h in the presence of isopropanol (a) and in the absence of isopropanol (b). Obviously, during the same reaction time, crystal nucleus of TG-1 is much smaller than that of TG-2.

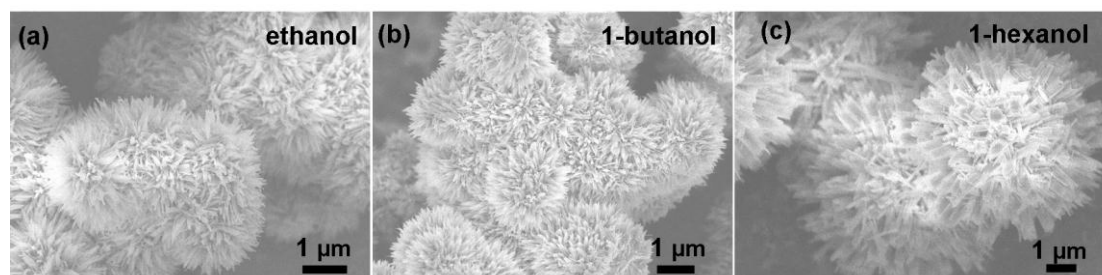


Fig. S7 SEM images of titanium glycerolates obtained in the presence of (a) ethanol, (b) butanol and (c) hexanol. From the above images, it is seen that ethanol and butanol with a low viscosity also lead to the formation of titanium glycerolates spheres composed of nanobelts, but hexanol with a high viscosity cannot lead to the morphology change of titanium glycerolate in comparison with pure glycerol system (the morphology is similar to TG-2).

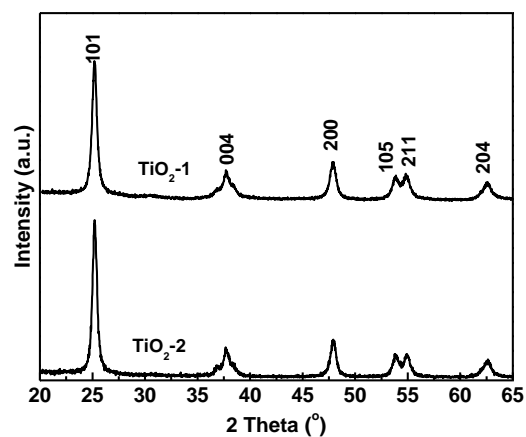


Fig. S8 XRD patterns of TiO₂-1 and TiO₂-2.

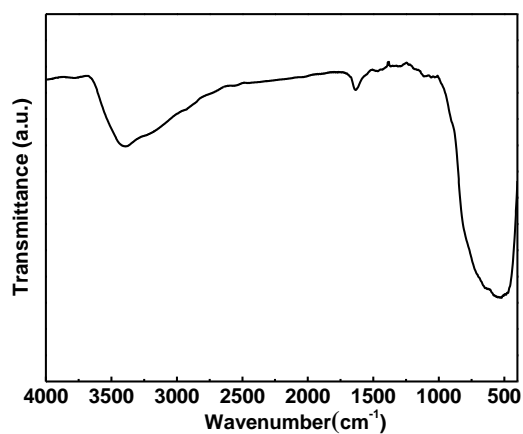


Fig. S9 IR spectrum of TiO₂-1.

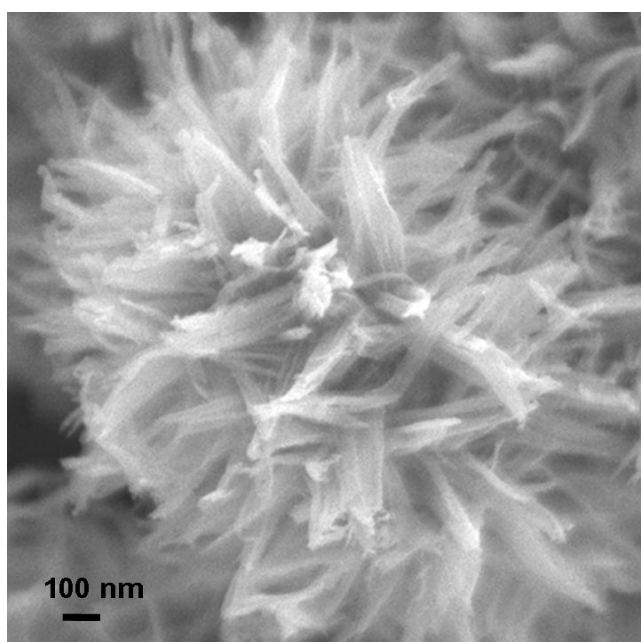


Fig. S10 High-magnification SEM image of TiO₂-1.

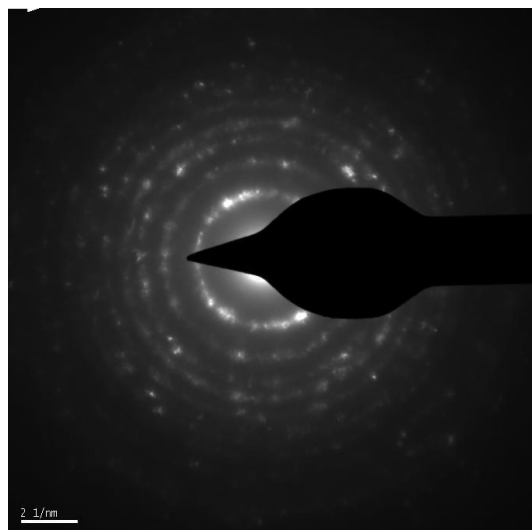


Fig. S11 The SAED image of TiO₂-1.

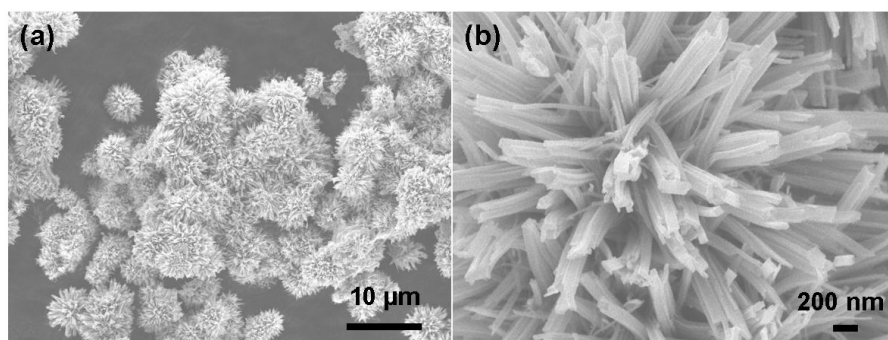


Fig. S12 SEM images of TiO₂-2.

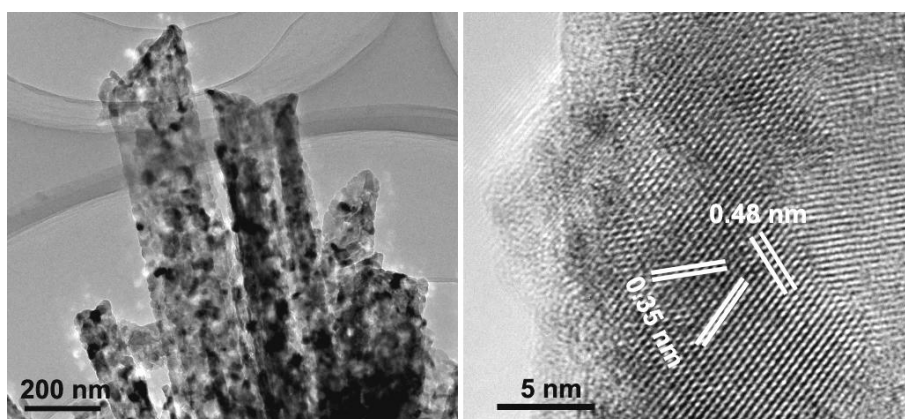


Fig. S13 TEM (left) and HRTEM (right) images of TiO₂-2.

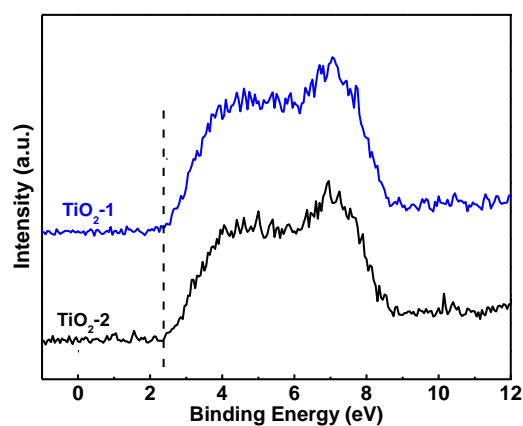


Fig. S14 Valence-band XPS spectra of TiO₂-1 and TiO₂-2.

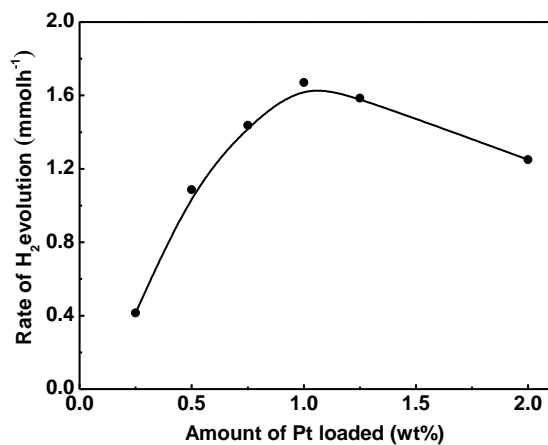


Fig. S15 The influence of Pt-loading amount on the H₂ evolution rate of TiO₂-1.

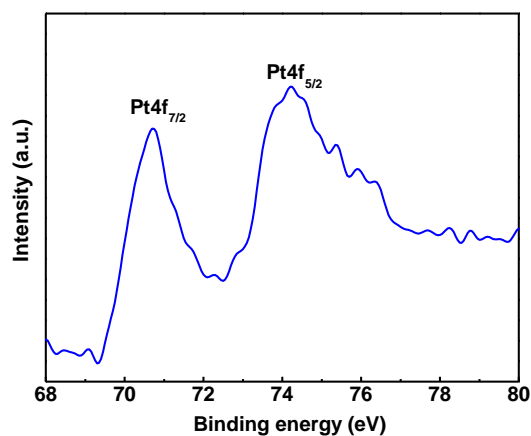


Fig. S16 The Pt4f XPS spectrum of Pt-modified TiO₂-1. The Pt4f XPS spectrum for Pt-modified TiO₂-1 exhibits two peaks at 70.7 and 74.2 eV, which are assigned to the Pt 4f_{7/2} and Pt 4f_{5/2} core level of metallic Pt, respectively.

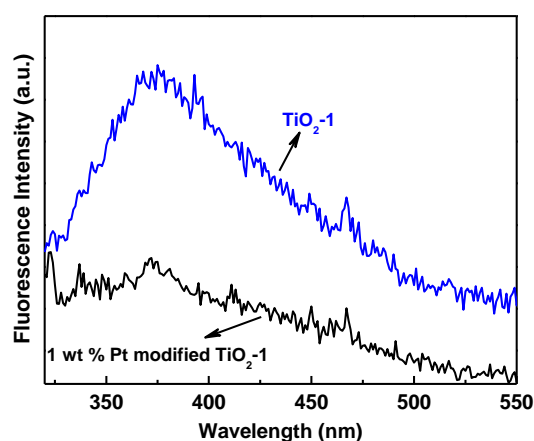


Fig. S17 The PL emission spectra of $\text{TiO}_2\text{-1}$ and 1 wt % Pt modified $\text{TiO}_2\text{-1}$.

Table S1 Viscosity of Various Organic Substances (Lange's Chemistry Handbook Version 15th)

Substance	Viscosity ($^{\circ}\text{C}$) $\text{mN} \cdot \text{s} \cdot \text{m}^{-2}$
Glycerol	934 (25)
Isopropanol	1.765 (30)
Ethanol	1.074 (25)
1-butanol	2.948 (20)
1-hexanol	3.872 (30)

Supporting Information References

S1. J. Das, F. S. Freitas, I. R. Evans, A. F. Nogueirab and D. Khushalani, *J. Mater. Chem.*, 2010, **20**, 4425.